SOILS AND FOUNDATIONS Vol. 47, No. 1, 153–160, Feb. 2007
Japanese Geotechnical Society

FAILURE OF REINFORCED EARTH AS ATTACKED BY TYPHOON NO. 23 IN 2004

SATORU SHIBUYA[i], TAKAYUKI KAWAGUCHI[ii] and JONGGIL CHAE[iii]

ABSTRACT

In October 2004, Typhoon No. 23 attacked western part of Japan, causing severe damage to infrastructures over a wide area in Kansai. In the early morning on 21st October, failure of a large Reinforced Earth wall with the maximum height of about 23 m took place in a mountainous area in Yabu city, Hyogo Prefecture. The debris flow from the reinforced embankment attacked a warehouse at the foot of the mountain, however, no casualties were reported. Immediately after the incident, an investigation committee was set up with missions to investigate the causes of this catastrophic embankment failure and also to examine any possible occurrence of further slope disasters in this region. In this paper, the failure mechanism by considering causes of the slope failure is discussed based on the results of stability analysis performed using laboratory and field data, coupled with topological information and the rainfall data. Some lessons learnt from this unique case study are described with reference to the design and construction of Reinforced Earth wall in rainy mountainous areas, in particular.

Key words: design, in-situ test, laboratory test, Reinforced Earth, shear strength, slope disaster (**IGC**: B5/B11/C3/D6/E6/H6)

INTRODUCTION

The design and construction manual of Reinforced Earth Armée wall does not consider any water in and adjacent to the reinforced soil. Similarly, little attention is paid to infiltration of rainfall water from the surrounding area. Nevertheless, the Reinforced Earth using metal strips has been popular in use for constructing local roads in mountainous area in Japan, where the attack of seasonal heavy rainfalls is commonly encountered. Moreover, when considering the need for reducing the construction cost, local government is often obliged to use local soils with low permeability and low friction angle in constructing Reinforced Earth wall. Despite that the stability of reinforced walls is usually threatened by rainfalls (e.g., *see* Kutara et al., 1991), a proper drainage system around the wall tends to be optional, not obligatory, in the light of the current format of the design and construction manual for this type of wall. Geotechnical engineers have therefore been concerned with the short-term stability of Reinforced Earth in the event of annual typhoon attacks as they are constructed in a mountainous region. Unfortunately, such a worry became a reality in the case study described in this paper.

At around 1:40 am on 21st of October 2004, a huge landslide involved with a catastrophic failure of Reinforced Earth wall took place in the mountainous area of Yabu city in northern part of Hyogo Prefecture in west Japan. The time of occurrence of the incident was quite exact by the record of an emergency phone call from a local resident to Yabu local government office. Figure 1 shows a picture of the wall failure that was taken a few months after the incident.

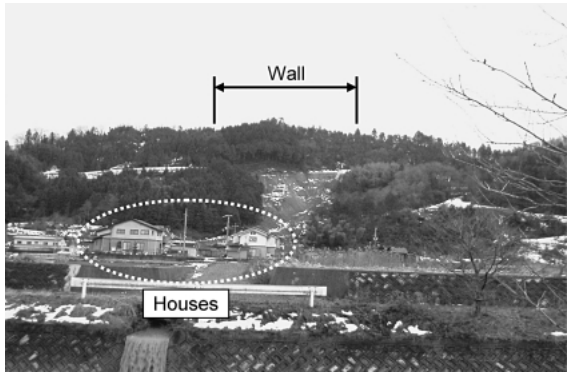

Fig. 1. Site after the collapse of Reinforced Earth wall

The urgent matter that after required attention was to ensure short-term safety of neighboring inhabitants against occurrence of any further slope disasters. Accordingly, under the authority of Yabu city government, comprehensive geotechnical site investigation was carried out over six-month period after the incident.

[i] Professor, Department of Architecture and Civil Engineering, Kobe University, Japan (sshibuya@kobe-u.ac.jp).
[ii] Associate Professor, Department of Civil Engineering, Hakodate National College of Technology, Japan.
[iii] Graduate Student, Graduate School of Natural Science, Kobe University.
The manuscript for this paper was received for review on May 9, 2006; approved on November 17, 2006.
Written discussions on this paper should be submitted before September 1, 2007 to the Japanese Geotechnical Society, 4-38-2, Sengoku, Bunkyo-ku, Tokyo 112-0011, Japan. Upon request the closing date may be extended one month.

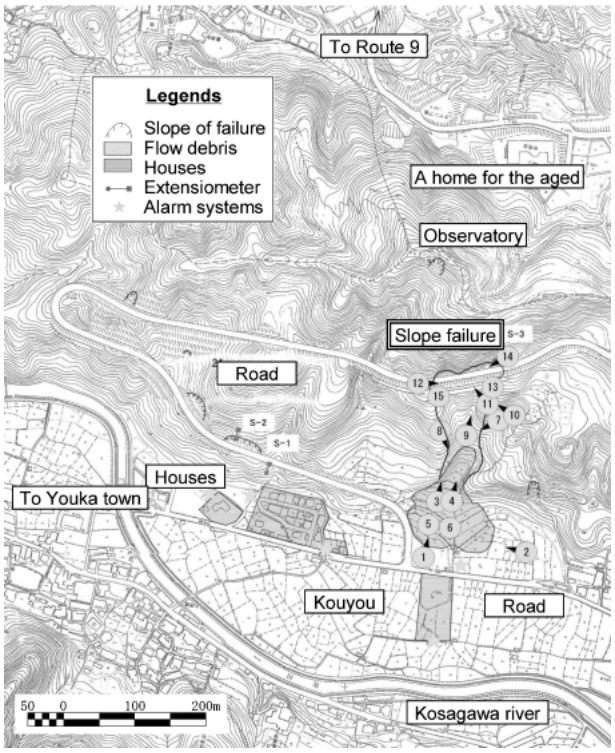

Fig. 2. Topographical map of the site immediately after the incident

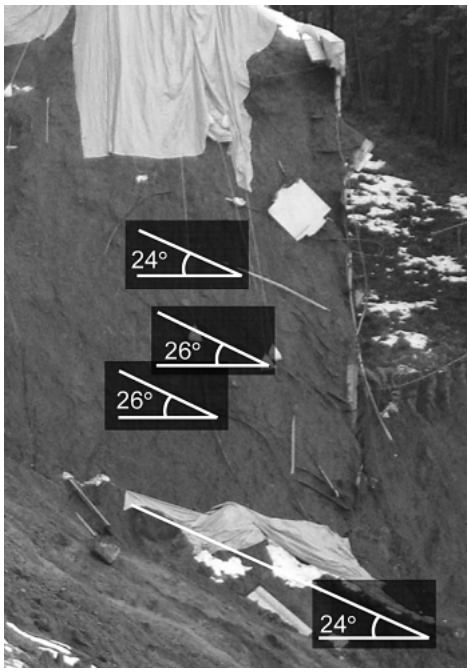

Fig. 3. Cross section of the remainder of the wall

In addition, in an attempt to back-analyze properly the stability of the collapsed wall, a series of direct shear box tests in simulating the mode of undrained shear of the foundation soil was carried out in the Geotechnical Engineering Laboratory at Kobe University.

In this paper, based on the results of geotechnical site investigation, key factors responsible for the wall collapse are manifested, and the scenario of the wall failure is discussed in depth by performing a conventional stability analysis with detailed soil profile and the strength data of the local soil.

OUTLINE OF THE WALL FAILURE

The construction of the reinforced wall was completed in the year of 2000, i.e., four years before the incident. Figure 2 shows a topographical map of the site showing the condition immediately after the failure of the wall. The numbers shown in this figure refer to spots from where some pictures immediately after the incident were taken in order to obtain any clues into the failure mechanism (Shibuya and Kawaguchi, 2006). The landslide took place over a length of about 150 m along the slope involved with the collapse of the wall over 80 m length along the road. It was obvious in the map that the slope over which the wall failure occurred consisted of a couple of small valleys. Moreover, the road was inclined about 7% from West (right hand side in Fig. 2) to East (left hand side in Fig. 2). These topographical surroundings would have brought about some concentration of surface/ground water into the collapsed portion of the road during the heavy rainfall.

Several key observations from comprehensive survey performed immediately after the incident (Shibuya and Kawaguchi, 2006) are:

i) Parts of the wall (i.e., concrete skins and metal strips) reached to the end of debris flow,
ii) Neither damage of metal skins nor breakage of metal strip/concrete skin joints was found,
iii) The remainder of the wall stood in good shape,
iv) The metal strips remaining on the side wall of wall were all inclined at an angle of 24–26 degrees from the horizontal that was equal to the supposed slip surface angle on the foundation (Fig. 3), and
v) Rainfall water poured into the collapsed area during rainfall.

Regarding the remark iv), it was observed that the metal strips in the remained wall aligned horizontally just like the arrangement when the wall was constructed. It should be mentioned that the collapsed wall was as high as 23 m. To the authors' best knowledge, such a huge collapse as that of Reinforced Earth wall has not been reported in the literature.

RAINFALL RECORD

As mentioned earlier, the incident took place at 1:40 am on 21st October in 2004. Figure 4 shows the intensity of rainfall with time over three days before and after the incident. It should be mentioned that the data was recorded at an observatory very close to the site. Heavy rain with the intensity in excess of 10 mm per hour continued over eight hours (1 pm–8 pm) on 20th October. Note that the amount of 226 mm of rainfall was certainly the peak record over the past eight years in this region. It may well be postulated that this heavy rainfall was the trigger of the disaster.

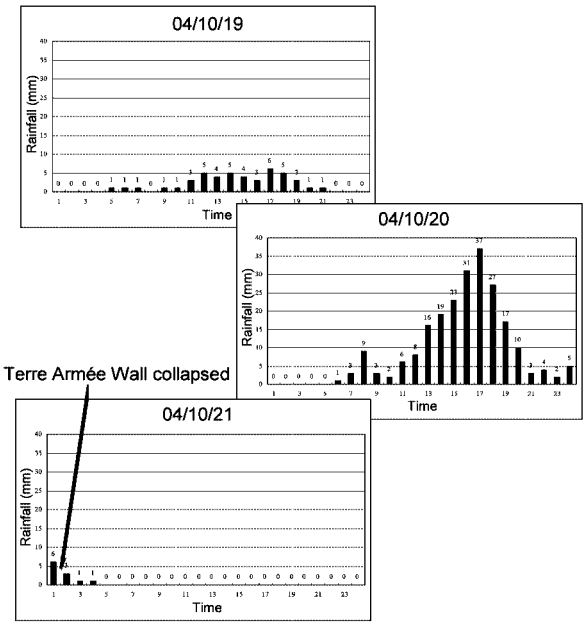

Fig. 4. Rainfall data

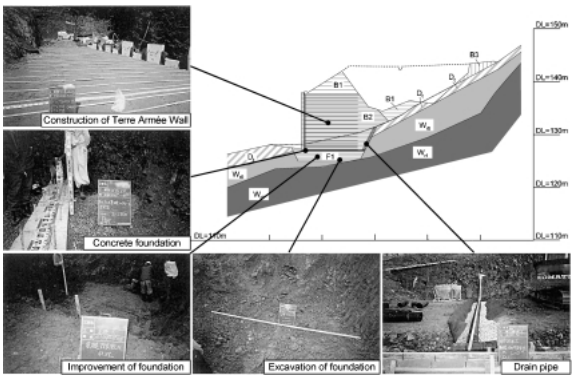

Fig. 5. Construction sequence of the wall

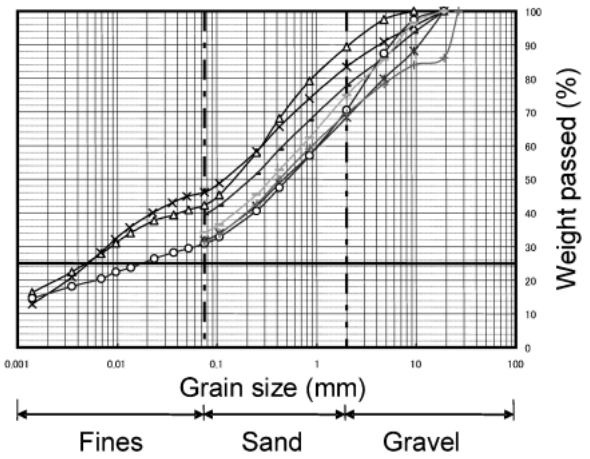

Fig. 6. Grain size distribution of soil

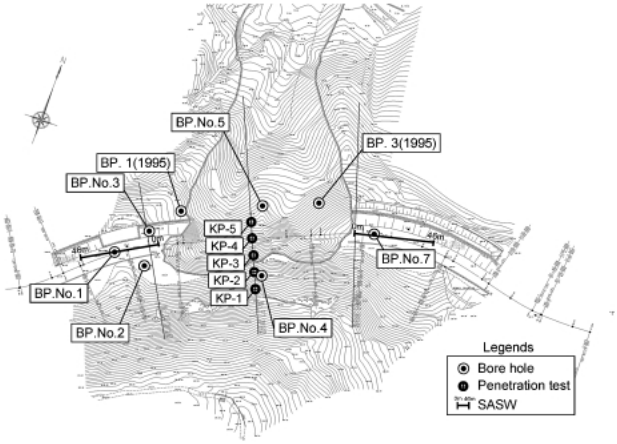

Fig. 7. Geotechnical site investigation performed

REINFORCED EARTH WALL COLLAPSED

Figure 5 shows the sequence of construction of this wall in the year of 2000. Some features pertaining to the design and construction of the wall are summarized in the below (Shibuya and Kawaguchi, 2006):

i) Local geomaterials, i.e., weathered silty soil originated from yellow tuff, with the fines content well in excess of 25% was employed for constructing the wall, noting that Fig. 6 shows the distribution curve of several samples from B2 layer,
ii) Drain pipe with a small diameter of 200 mm was employed at the bottom of the wall, but it did not extend to cover an area behind the wall (*see* Fig. 5),
iii) The surface of the road had been unpaved over the past four years, and
iv) SPT *N*-value in the foundation ranged between 15 and 20, which was surprisingly low to support the soil wall with the maximum height of 23 m.

It should be mentioned that in the construction of the wall, the local soil was mixed with cement-based stabilizer in order to secure prescribed friction between metal strips and the soil. As stated later, the soil stabilization treatment has reduced the permeability of in-wall soil to a considerable extent.

GEOTECHNICAL SITE INVESTIGATION

Sounding

The site is covered with heavily weathered soil originated from yellow tuff. Geotechnical site investigation performed is shown in Fig. 7. The scheme consisted of SPT sounding and in-situ seismic survey to cover the survived as well as the collapsed portions of the wall. The SPT sounding along three survey lines from south to north involved with soil sampling by using the Japanese thin-wall sampler. Spectrum analysis of surface wave (SASW) (Stokoe et al., 1988) was also carried out at the survived parts of the wall.

Cross sections of the wall depicted from these geotechnical investigations are shown in Fig. 8. As seen in Fig. 8, the subsoils may be conveniently characterized into seven layers as described below:

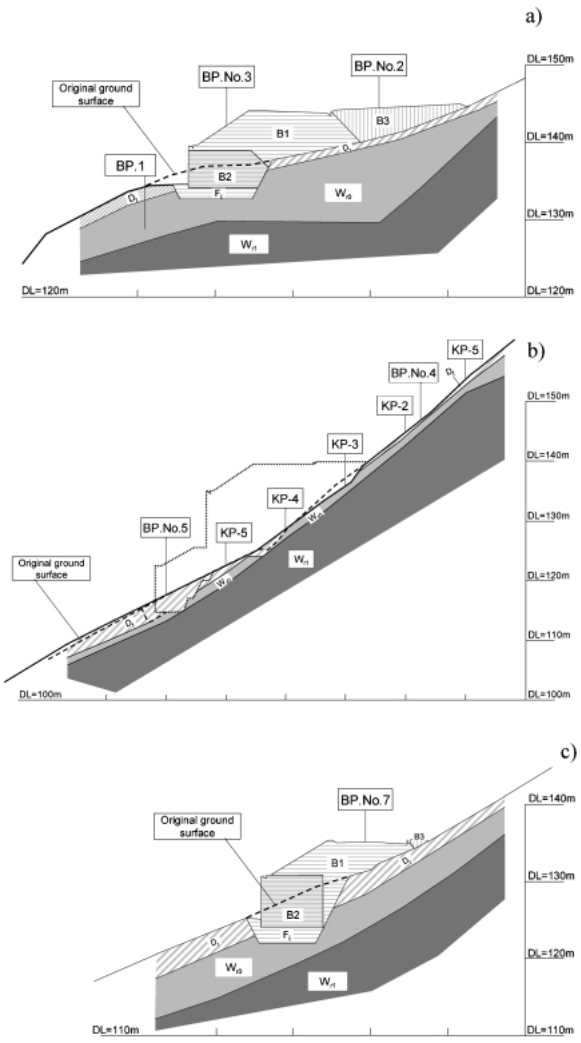

Fig. 8. Cross section of the wall: a) west line, b) central line and c) east line

Road Embankment

i) Surface layer (B1-layer) with the SPT N-value ranging from 1 to 11 ($N=5$ on average), non-uniform and the fines content ranged from 30 to 80%,

ii) Improved layer (B2-layer) with the SPT N-value ranging from 15 to 18 ($N=16$ on average), relatively uniform and the fines content ranged from 31 to 46%,

iii) Behind the wall layer (B3-layer) with the SPT N-value ranging from 2 to 5 ($N=4$ on average), non-uniform and comprising gravel-size particles about 30–40% by weight, and

iv) Base layer (F_i-layer) with the SPT N-value average of 17.

Surface Soil/Foundation

i) Surface soil (D_t-layer) with the SPT N-value ranging from 3 to 5 ($N=4$ on average)

ii) Weathered rock layer (W_{r0}-layer) with the SPT N-value ranging from 5 to 50 ($N=22$ on average), and a clear trend of N-value to increase with depth, and

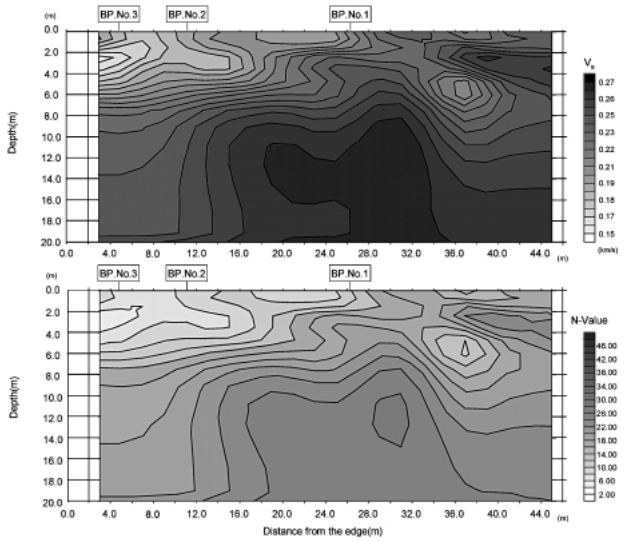

Fig. 9. Profile of shear wave velocity from SASW method (west side)

iii) Foundation rock (W_{r1}-layer) with $N>50$.

It is to be noted that the wall rests on W_{r0}-layer with N-value of 22 on average. It should also be mentioned that the permeability from in-situ test was in the order of 10^{-5} (m/s) for weathered rock layer (W_{r0}-layer), whereas it was smaller by one order of magnitude in the road embankment (i.e., B1, B2 and B3 layers).

Spectrum Analysis of Surface Wave (SASW)

SASW survey is a non-destructive method by which the profile of shear wave velocity, V_s, with depth is easily manifested down to the depth of about 20 m. Figure 9 shows the result of the survey performed at west end of the remaining wall (*see* Fig. 7). In this figure, the N-value estimated using the following empirical expression is also shown for comparison.

$$N=(V_s/b)^a \tag{1}$$

where the constants, $a=0.314$, $b=97$ (m/s) were employed (Imai et al., 1975).

The following may be noted:

i) The shear wave velocity, V_s, ranged from 150 m/s to 360 m/s as examined down to depth 20 m,

ii) The profile of estimated N-value using Eq. (1) is similar to the measurement, indicating that the N-value of weathered rock (W_{r0}-layer) is far less than 50 throughout the layer.

The efficacy of the SASW method was well demonstrated in this investigation that it provided 2-D picture of N-value profile with depth, from which the soil layering shown in Fig. 8 was determined with reasonable confidence.

Laboratory Shear Tests

Two kinds of laboratory tests were performed in order to obtain soil strength in use for back-analyzing the wall failure. In the first place, a series of unconsolidated-undrained triaxial compression tests (i.e., triaxial UU test) was carried out using intact samples from different

Table 1. Soil properties

Depth GL-m	Bulk density ρ_t (g/cm^3)	Dry density ρ_d (g/cm^3)	Soil particle density ρ_s (g/cm^3)	Natural water content ω_n (%)	Void ratio e	Degree of saturation S_r (%)
5.0–5.7	1.831	1.322	2.737	38.5	1.071	98.5
7.0–8.0	1.816	1.321	2.727	37.4	1.064	95.9
2.0–2.6	1.634	1.205	2.716	35.7	1.261	77.6
3.0–3.7	1.888	1.468	2.768	28.7	0.887	89.7
0.5	1.723	1.203	2.708	43.2	1.251	93.5

Table 2. Results of triaxial UU test

Soil layer	Bulk density ρ_t (g/cm^3)	Total stress		
		c (kPa)	ϕ (°)	tan ϕ
B2 and F_i	1.8	46.3	7.77	0.136
B1 and B3	1.7	68.0	3.66	0.064
D_t	1.6	41.9	14.96	0.267
W_{r0}	1.8	36.4	12.08	0.214

depths. The results are shown in Table 1 and Table 2. Note that the soil samples from not only embankment but also the foundation were all close to full saturation. As a result, the angle of shear resistance ϕ from triaxial UU test was small with the values less than 10 degrees. The cohesion, c, was 46 kPa and 68 kPa for improved layer (B2) and unimproved layer (B3), respectively.

Secondly, two series of constant-volume direct shear box tests were performed using reconstituted samples retrieved from the slip surface. A block sample was first prepared from the slurry with the initial water content approximately equal to liquid limit (i.e., 50–60%). Figure 10 shows the direct shear box apparatus developed at Hokkaido University (Shibuya et al., 2001). The load control as well as data acquisition is fully automated with an aid of PC. The nominal dimension of the specimen was 6 cm in diameter and 4 cm high. The gap between the upper and lower shear boxes was maintained at a constant value of 0.5 mm during shear, noting the mean diameter of about 0.1 mm for the soil tested. The soil density was 1.7–1.8 g/cm^3 being very close to the in-situ density.

Regarding a sketch shown in Fig. 11, three samples in the first series were each consolidated to the vertical consolidation stress, σ_{vc} of about 200, 300 and 400 kPa, respectively. Afterwards, the samples were sheared under constant-volume conditions by using a constant rate of horizontal displacement of 2 mm/min. The undrained effective stress paths of this conventional consolidated-undrained (CU) test are shown in Fig. 12, in which the variation of normal (=vertical) effective stress is plotted against the horizontal shear stress, τ. The effective strength parameters of $(c', \phi') = (0, 37.4°)$, together with the total stress parameters, $S_u/\sigma_{vc} = 0.34$ were obtained

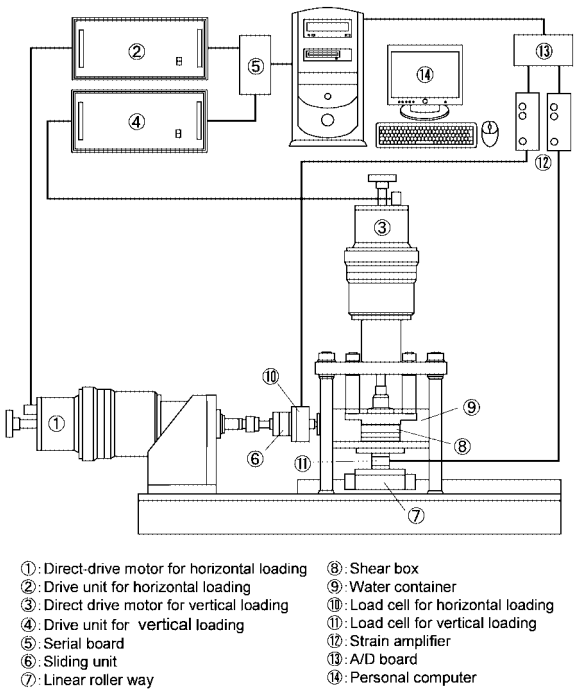

Fig. 10. Direct shear box apparatus

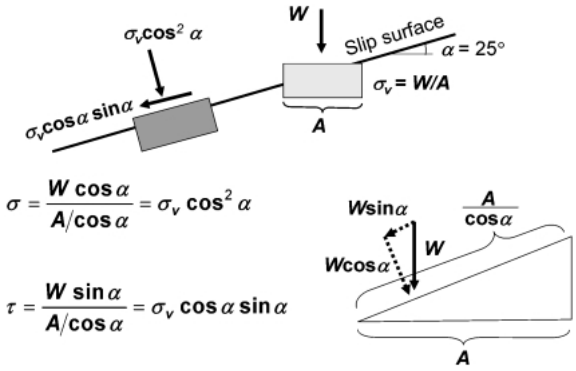

Fig. 11. Stress conditions along the slip surface

for the long-term and short-term stability analysis, respectively. In the second series, in-situ stress conditions on the collapsed slope were more closely simulated in each sample by applying initial shear stress under drained conditions (refer to Fig. 11). In general, in-situ soil element on a slope with angle α from the horizontal is subjected to the initial stress conditions as shown in the following;

$$\sigma_i = \sigma_{vc} \cos^2 \alpha \tag{2}$$

$$\tau_i = \sigma_{vc} \cos \alpha \sin \alpha \tag{3}$$

Figures 13 and 14 show the results of five tests performed in the second series. As can be seen in Fig. 13, each sample was first consolidated to a prescribed initial (and common) vertical stress of $\sigma_i = 246$ kPa ($= 300 \times \cos^2 25°$), where the angle of 25° corresponds to the averaged angle of the collapsed slope from the horizontal (*see* Fig. 3). The sample was then subjected to application of drained initial shear to the value of $\tau_i = 115$ kPa ($= 300 \times$

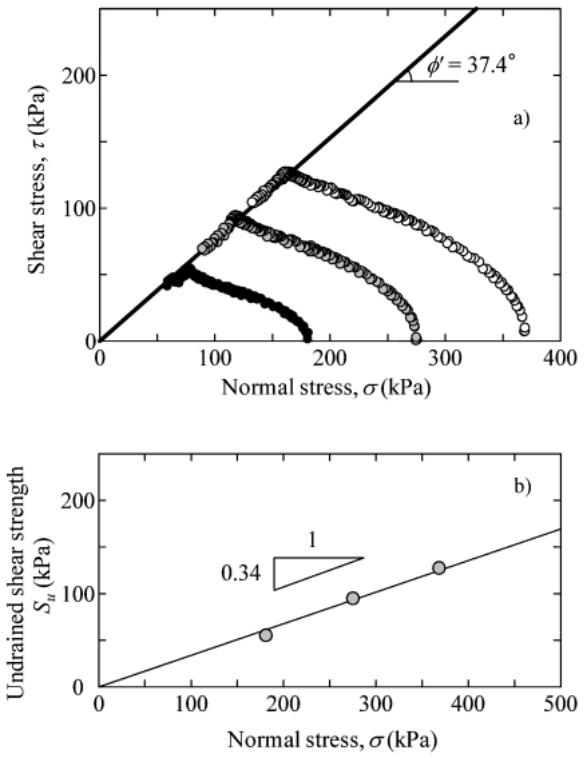

Fig. 12. Results of conventional direct shear test: a) effective stress paths and b) undrained shear strength

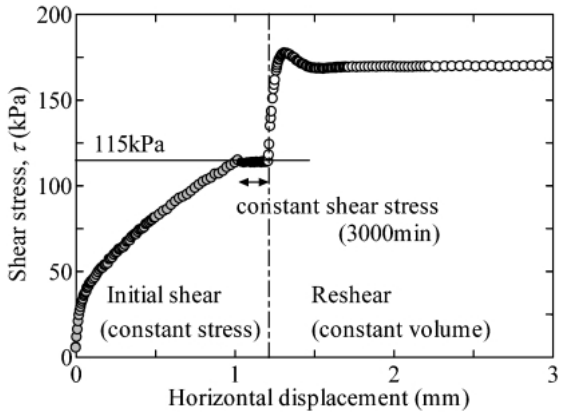

Fig. 13. Relationship between horizontal shear stress and horizontal displacement in a test with initial shear

cos 25° sin 25°) by using a slower rate of horizontal shear displacement of 0.02 mm/min. The initial shear stress was then maintained constant over a prescribed period in each test. At this initial shear stage, the volume change of the sample was insignificant whereas the horizontal shear displacement developed as much as 0.2 mm (*see* Fig. 13). The sample was finally sheared to failure under the conditions of constant volume by using a faster rate of 2 mm/min. The initial shear stress was maintained over different, but fixed, periods of 1, 10, 100, 3,000 and 10,000 min, respectively. Surprisingly, the effective stress path was very much influenced by the duration of the initial shear stress application, showing that it rose more sharply as the duration increased (*see* Fig. 14). As a

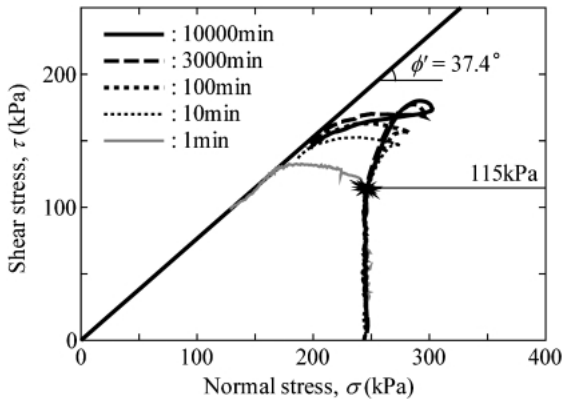

Fig. 14. Undrained effective stress paths in direct shear box test with initial shear

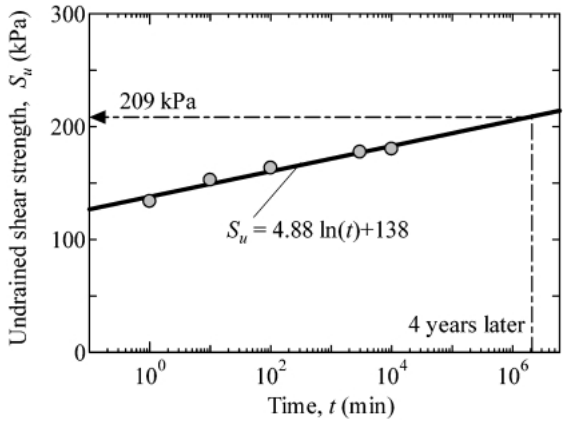

Fig. 15. Undrained shear strength versus duration of initial shear stress applied

consequence, the undrained shear strength S_u (i.e., the maximum shear stress) also increased with the sustained period of initial shear stress. On the other hand, the effective strength parameters of $(c', \phi') = (0, 37.4°)$ were not affected at all by the application of initial shear (refer to Fig. 12). The significant softening behavior observed in the second series suggests strongly that a catastrophic type of failure would take place once the foundation soil exceeds the peak strength.

Figure 15 shows the S_u value in the second series when examined against the sustained period of initial shear. Bearing in mind that the wall collapsed at 4 years after the construction, the value of 209 kPa for $\sigma_{vc} = 300$ kPa, hence $S_u/\sigma_{vc} = 209/300 = 0.70$, was attained by extrapolating the S_u values from the laboratory test to an instant after 4 years.

SCENERIO OF THE WALL FAILURE

Based on the field observations, the results of geotechnical investigation and comprehensive review of design and construction scheme of the wall, it was concluded that this particular wall was properly designed and constructed in the light of the available ''design and

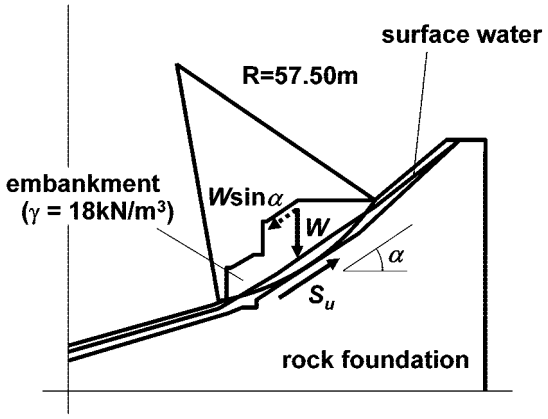

Fig. 16. Short-term stability analysis

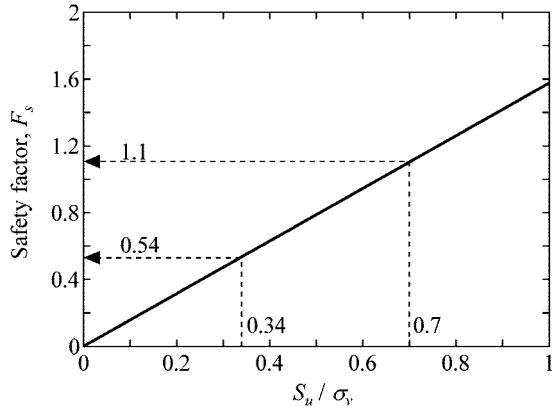

Fig. 17. Back calculated factor of safety with S_u/σ_{vc}

construction manual'' (Civil Engineering Research Center, 2003). However, it is the fact that the wall failed due to the heavy rainfall.

The wall failure may be attributed to simultaneous occurrence of several, not a single, causes as listed below:

i) Concentration of in-soil seepage and surface water flow into the collapsed area,
ii) Relatively low permeability of embankment (B1, B2 and B3 layers) as compared to the weathered rock foundation (W_{r0}-layer) (*see* Fig. 8),
iii) Poor drain system behind the wall in particular,
iv) Low bearing capacity of the foundation, and
v) Softening characteristic of the foundation soil as sheared undrained (*see* Figs. 13 and 14).

It should be stressed that the first three possible causes have something to do with problems of in-soil seepage flow. As stated earlier, according to ''design and construction manual'' in Japan like in other countries perhaps, any existence of water/water flow is not considered at all in the design of the wall. In fact, however, rainfall water invaded the reinforced embankment in this case study. It was confirmed with the result of field observation that the degree of saturation of the collapsed embankment soil was nearly equal to 100% when examined right after the incident.

The short-term stability analysis assuming circular slip surface was carried out by using the strength parameters from triaxial UU test and constant-volume direct shear test. Figure 16 shows the short-term stability analysis performed at the central portion of the collapsed wall (*see* Fig. 8(b)). The surface water level was postulated based on in-situ measurement that was made immediately after the incident. The results of back-analysis are shown in Fig. 17, in which the back-calculated factor of safety, F_s, is plotted against the total stress strength parameter, S_u/σ_{vc}. Note that F_s is close to unity (i.e., $F_s = 1.1$) when the S_u/σ_{vc} value of 0.70 is employed, whereas F_s was far less than unity when S_u/σ_{vc} of 0.34 from conventional direct shear test is used for the calculation. The result strongly suggests that we should use soil strength from direct shear box test in which the magnitude as well as history of initial stress conditions on the supposed slip surface are closely simulated in the laboratory. In the stability analysis performed, it was assumed that the soil behind the wall was saturated as a consequence of heavy rainfall over a short period of time. The effect of concentrated rainfall on the wall stability was manifested in the fact that the F_s value with dry soil (i.e., $S_r = 0\%$) behind the wall was far greater than unity.

Regarding the sketch shown in Fig. 18, the scenario of the wall failure could be described as:

i) A great deal of in-soil and surface water poured into the collapsed area over a short period of time,
ii) The water infiltrated into the embankment and gradually stored behind the wall since the permeability of the wall was relatively small,
iii) Total load increased due to the water infiltration,
iv) Seepage water pressure in the weathered rock foundation having relatively high permeability increased gradually,
v) The overall stability of the embankment reduced substantially due to the water storage in and behind the wall, together with possible development of seepage pressure in the foundation soil,
vi) The localized failure on the foot of the wall may have occurred due to the lack of bearing capacity, and
vii) A type of circular slip occurred across the foundation.

The wall failure as such could be described simply as ''the undrained shear failure of foundation since the wall acted as if a reservoir dam in the event of heavy rainfall''. Finally, it is strongly recommended that the design and construction manual should be revised properly so as to prevent any future occurrence of this type of failure. The case study described in this paper also suggests the strong need for co-operation between structural engineers and geotechnical engineers.

CONCLUSIONS

The Reinforced Earth wall that collapsed was properly designed and constructed in the light of ''design and construction manual'' in Japan. Unfortunately, it was a fact that the wall failed during the heavy rainfall as

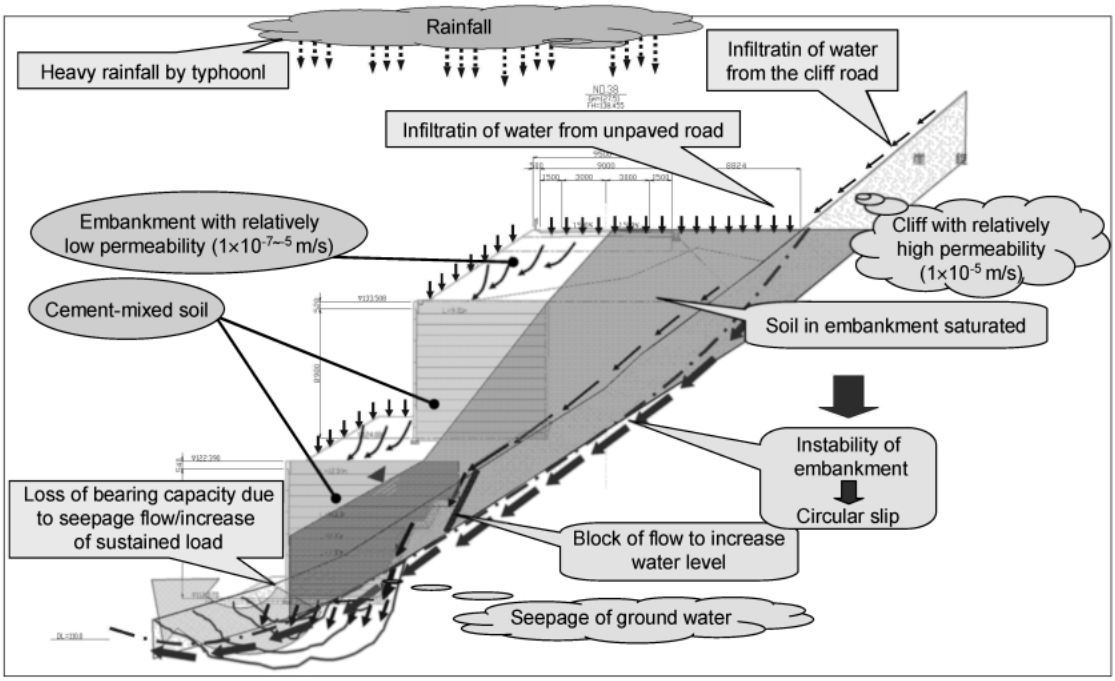

Fig. 18. Scenario of the wall failure

attacked by Typhoon No. 23 in October, 2004.

Field observations immediately after the incident coupled with the result of the stability analysis corroborated the premise that the wall itself stood in a good shape till the moment of the catastrophic failure. The wall failure in this case study could be described simply as ''the undrained shear failure of foundation'' since the wall acted as if a reservoir dam in the event of heavy rainfall. Simultaneous occurrence of several causes such as concentration of in-soil seepage and surface water flow into the collapsed area, low permeability of embankment, poor drain system behind the wall, etc. were supposedly responsible for the failure. It is therefore recommended that the design and construction manual should be revised properly so as to prevent any future occurrence of this type of failure induced by heavy rainfalls. In so doing, every effort should be made to prevent water from seeping into and near the wall.

Other lessons learnt from this unique case study are:

i) Drainage system should take care not only the wall but also the embankment behind the wall,
ii) The wall should be placed on rock foundation with SPT *N*-value more than 50,
iii) The surface of the road should be temporarily paved even in the course of construction by which infiltration of surface water into the surroundings of the wall may be grossly lessened, and
iv) In short-term stability analysis of the wall involving the case of rainfall attacks, it is promising to employ soil strength from direct shear box test, in which the magnitude as well as history of initial stress conditions on the supposed slip surface are closely simulated, and
v) Construction of this type of Reinforced Earth wall needs sound co-operation between structural engineers and geotechnical engineers.

ACKNOWLEDGEMENT

Most of field data reported in this paper is referenced to the report issued by the technical committee of Yabu city chaired by Professor Makoto Nishigaki, Okayama University.

REFERENCES

1) Civil Engineering Research Center (2003): *Design and Construction Manual of Reinforced Soil Wall Method* (in Japanese).
2) Imai, T., Roku, H. and Yokota, K. (1975): Relationship between shear wave velocity and mechanical properties of Japanese soils, *Proc. 5th Symp. Earthquake Engineering* (in Japanese).
3) Kutara, K., Miki, H., Nakayama, K. and Fujiki, H. (1991): Behavior of prototype steep slope embankment having soil-walls reinforced by continuous fibers, *J. Construction Management and Engineering*, JSCE, (427, VI-14), 223–232 (in Japanese).
4) Shibuya, S., Mitachi, T., Tanaka, H., Kawaguchi, T. and Lee, I. M. (2001): Measurement and application of quasi-elastic properties in geotechnical site characterisation, *Theme Lecture, Proc. 11th Asian Regional Conference on SMGE*, Seoul, Balkema, **2**, 639–710.
5) Shibuya, S. and Kawaguchi, T. (2006): Lessons learnt from a catastrophic failure of terre armée wall due to heavy rainfall, *Geomechanics II, Proc. Second Japan-U.S. Workshop on Testing, Modeling and Simulation in Geomechanics*, ASCE, Kyoto, 454–470.
6) Stokoe, K. H., Nazarin, S., Rix, G. J., Sanchez-Salinero, I., Sheu, J. C. and Mok, Y. J. (1988): In situ seismic testing of hard-to-sample soils by surface wave method, *Earthquake Engineering and Soil Dynamics II, Recent Advances in Ground Motion Evaluation*, ASCE, 264–278.